

Dynamic Stark Effect of Exciton and Continuum States in CdS

N. Peyghambarian, S. W. Koch,^(a) M. Lindberg, B. Fluegel, and M. Joffre^(b)

Optical Sciences Center, University of Arizona, Tucson, Arizona 85721

(Received 10 August 1988; revised manuscript received 3 November 1988)

The first observation of the optical Stark effect of electron-hole continuum states in addition to the bound-exciton states is reported under femtosecond excitation conditions chosen to minimize the generation of real carriers. The experimental results agree well with calculations using the generalized semiconductor Bloch equations. The theory shows that the commonly used adiabatic approximation is correct only for pulses which are longer than the coherence decay time. For shorter pulses coherent dynamic effects strongly influence the spectral changes.

PACS numbers: 71.35.+z, 71.70.Ej

The optical Stark effect is a well-known phenomenon in atomic systems where an atomic transition shifts by application of an off-resonance light beam.¹⁻³ The effect persists for the duration of the optical pulse and has been explained using the "dressed atom" picture. In semiconductors, one deals with a combination of bound electron-hole-pair (exciton) resonances and unbound continuum states. The optical Stark effect of excitons in multiple quantum wells and in Cu₂O has been observed recently.⁴⁻⁸ However, the Stark effect of continuum states has not yet been reported.

Quite generally, there is always a competition between effects caused by real carriers and the electric field effects (Stark effect) in semiconductors which often complicates the observation of a "pure Stark effect." Even when the light frequency is detuned from the resonance such that one-photon carrier generation is very small, two-photon absorption may lead to a finite concentration of real excitations. These carriers affect the exciton through many-body interactions, leading to energy renormalizations, bleaching, and broadening of resonances. In order to minimize these long-lived effects (real excitations decay on the time scale of the interband recombination time) and to approach the regime of the true optical Stark effect, we have employed large detunings and weak excitation pulse intensities. Under these conditions, we observe not only the exciton shift but also the shift of unbound electron-hole continuum states for the first time. Our calculations, which fully take into account the coherent interaction of the light and the electron-hole excitations, agree well with the experimental results. In addition, it is shown that for pulses which are long in comparison to the medium coherence time a pure shift of the spectrum may be obtained, whose magnitude follows the square of the pulse amplitude.

For pulses shorter than the medium polarization dephasing time the evolution of the Stark effect is much more complex due to coherent dynamics of light-matter interactions as we have shown in our previous publication.⁹ For negative time delays ($t_p < 0$, probe preceding pump pulse) spectral oscillations may occur in the

differential transmission spectra (DTS), $= (T - T_0) / T_0$, where T and T_0 are the probe transmission in the presence and absence of the pump pulse. For detunings below the exciton resonance, the oscillations occur around the exciton as a consequence of the interference between the perturbed probe field and the pump-induced change in the transmitted probe field. As is emphasized in the theoretical analysis presented below, for $t_p \cong 0$ these oscillatory DTS features develop into the dispersive shape characteristic for the optical Stark shift. However, one has a "pure Stark shift" only for situations when the changes in the excitation pulse occur on time scales which are long in comparison with the medium coherence time, which is not realized under the present experimental conditions. Therefore, in the analysis, we have to consider all transmission changes caused by the total material-pulse interaction. We refer to the complete scenario of these differential transmission changes for the case of nonresonant excitation as the "optical Stark effect."

The experimental arrangement is a usual pump-probe technique. The output of a colliding-pulse mode-locked dye laser is amplified by a copper-vapor laser and the output is divided into two parts. One part goes through an ethylene glycol jet and produces a broadband continuum to be used as a probe pulse. The other part is sent through a delay generator and is used as a pump pulse with 60-fs duration (FWHM of the autocorrelation trace). A spectrometer and an optical multichannel analyzer detect the probe transmission as a function of frequency in the absence and presence of the pump and at various time delays between the pump and probe pulses.

In Fig. 1(a) we show the measured linear absorption spectrum of CdS at a temperature of 10 K. The valence band in CdS is split into three subbands giving rise to three excitonic levels labeled A , B , and C , respectively. The experiments are conducted using a probe polarization parallel to the crystal c axis, such that the A exciton is dipole forbidden and appears only as a shoulder on the low-energy side of the B exciton. Between the B - and

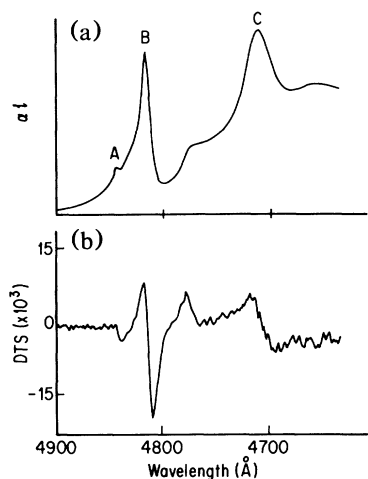


FIG. 1 (a) The linear absorption spectrum of CdS at 10 K for $E_p \parallel c$. (b) The measured DTS around zero time delay.

C-exciton resonances one sees the *B* band edge (electron-hole continuum and the unresolved higher *B*-exciton states) as a sharp kink. In Fig. 1(b) we show the DTS around zero time delay between pump and probe pulse. The Stark effect of all the excitons is observed as dispersive structures around the exciton resonances. Furthermore, the Stark effect of the *B* band edge is clearly seen as a positive DTS signal in the band-edge region.

Note that the dispersive structure around the *B*-exciton resonance in Fig. 1(b) is somewhat asymmetric. We attribute this feature to the asymmetry of the *B*-exciton line shape, which is specially pronounced at low temperatures [Fig. 1(a)]. This can be verified by measuring the DTS at slightly higher temperatures (100 and 150 K) where the additional phonon broadening makes the line shape much more symmetric, as can be seen from the linear absorption spectrum (inset to Fig. 2). Figure 2(a) shows the DTS around the *B* exciton and again the Stark effect of the *B* band edge. In Fig. 2(a), we have also plotted the spectrum obtained by artificially shifting the linear absorption and subtracting the resulting shifted curve from the unshifted curve. The good agreement between the two curves in Fig. 2(a) reveals that at low intensities and for large detunings one may obtain an almost pure Stark shift of the spectrum.

We studied the influence of the generated real carriers by monitoring the DTS for positive time delays, after the pump pulse has left the sample. In Fig. 3 we show the DTS around the *C* exciton for $t_p \cong 0$ and $+200$ fs. Clearly, at 200 fs the dispersive features have completely recovered and only a small longer-lived effect due to real carriers remains. However, these long-lived real excitations observed at later time delays do not contribute to the spectra at zero or negative time delays with the same strength. For two-photon absorption the carrier concentration follows the integral of the square of the pump

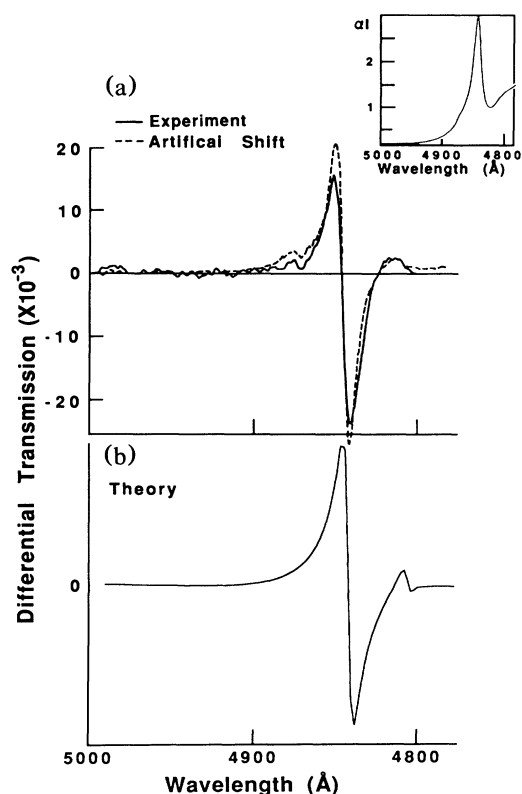


FIG. 2. (a) The measured DTS in the vicinity of the *B* exciton (full line) and its comparison with a pure shift of the absorption spectrum (dashed line) (see the text for description). (b) The calculated DTS in the vicinity of the *B* exciton for $t_p = -25$ fs and a pump pulse duration of 60 fs.

pulse, which reaches its maximum value after the pump pulse. At $t=0$, when the electric field of the pump pulse is maximum, the carriers reach at most half of their maximum value.

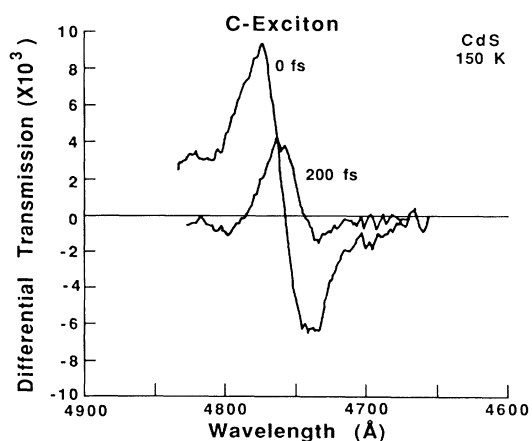


FIG. 3. The measured DTS in the vicinity of the *C* exciton at 150 K for the time delays of 0 and $+200$ fs.

The theoretical analysis of the observed transmission changes is done using the generalized semiconductor Bloch equations for the interband polarization $P(k)$ and the electron-hole densities $f_{e/h}(k)$ is derived by Lindberg and Koch.¹⁰ For the conditions in the discussed experiments, we assume that the exchange effects are small and can be neglected. However, the attractive part of the Coulomb interaction has to be taken into account. Using the s -type eigenfunctions $\psi_\lambda(x)$ of the electron-hole-pair Wannier equation, we introduce transformed variables P_λ and $f_{e/h,\lambda}$ which obey coupled equations having the form of the Bloch equations for an inhomogeneously broadened two-level system.¹⁰ These equations are solved for a given pump pulse and the total material polarization P_{tot} is obtained as

$$P_{\text{tot}} = \mu \sum_{\lambda} |\psi_{\lambda}(x=0)|^2 P_{\lambda} + \text{c.c.},$$

where μ is the interband dipole matrix element. From the total polarization we compute the material susceptibility and the pump-induced changes of the semiconductor transmission spectra.

Using only a single-exciton resonance and the parameters of CdS at $T=100$ K, we obtain the spectra shown in Fig. 2(b). Comparison with Fig. 2(a) reveals that the features observed in the experiment are recovered in the calculations. In Figs. 4(a)–4(c) we plot the computed DTS for different time delays and different temporal widths Δt of the pump pulses, such that the ratio $t_p/\Delta t$ is the same for the corresponding curves in Figs. 4(a)–4(c). The top curve in Fig. 4(b) is very similar to the result shown in Fig. 2(b). An analysis of Figs. 4(a)–4(c) shows that the magnitude of the transmission changes follows the square of the pump-pulse amplitude only for the 1-ps pulse. In this case the adiabatic approximation of Refs. 11–14 is justified. However, for the sample of a 10-fs pulse in Fig. 4(a), the magnitude of the transmission changes actually *decreases* slightly in the interval from $t_p = -25$ fs to $t_p = 0$. This behavior can be understood from the fact that the coherent changes in the differential transmission are only caused by the integral over the part of the pump pulse which enters the sample *after the probe pulse*. Clearly, as long as the coherence decay time is much longer than $|t_p|$, this integral—and therefore the pump-induced changes—is larger for larger negative time delays, i.e., for smaller pulse overlap.

In summary, we have presented an experimental and theoretical analysis of the optical Stark effect of exciton and continuum states in semiconductors for different delay times between pump and probe pulses. In the experiments we have minimized the effects of real carriers by choosing a large detuning and low intensity of the excitation pulse. The discussed theory includes the dynamic variations of the applied field and is in this respect an extension of the results presented in Refs. 11–14. It can be shown that the importance of coherent effects in the

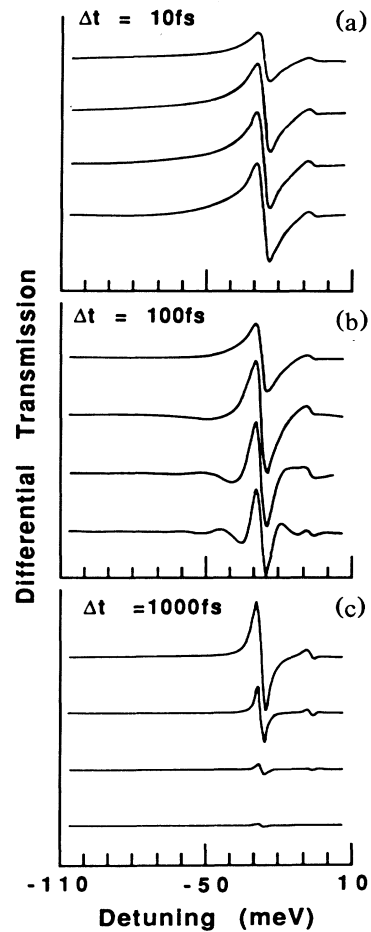


FIG. 4. The calculated DTS for three pulse widths: (a) $\Delta t = 10$ fs; (b) $\Delta t = 100$ fs; and (c) $\Delta t = 1000$ fs. The ratios of the time delays to the pulse width in (a)–(c) are kept the same. For all the parts the $t_p/\Delta t$ values are -2.5 , -1.6 , -0.8 , and 0 .

DTS decreases with increasing temporal pulse width. It should be noted that recently the Stark effect in the absence of real excitations was also seen in GaAs multiple quantum wells.¹⁵

The authors would like to acknowledge support from the Optical Circuitry Cooperative of the University of Arizona, the National Science Foundation (Grants No. EET8610170, No. EET8620265, and travel grant), Joint Services Optical Program (JSOP), NATO (travel grant No. 86/0749 and No. 87/0736), ONR–Strategic Defense Initiative Organization (SDIO) (Grant No. N00014-86-K-0719), U.S. Defense Advanced Research Projects Agency (DARPA)–Rome Air Development Center (RADC) (Grant No. F30602-87-C-0009), and the John von Neumann Computer Center for the computer time. We also acknowledge fruitful discussions with D. Hulin and A. Migus from Ecole Nationale Supérieure de Techniques Avancées (ENSTA), France.

Chirp correction and data acquisition programs were originally formulated by researchers at ENSTA.

^(a)Also at Physics Department.

^(b)Permanent address: Ecole Polytechnique, Ecole Nationale Supérieure de Techniques Avancées (ENSTA), Palaiseau, France.

¹C. Cohen-Tannoudji and S. Reynand, *J. Phys. B* **10**, 345 (1977).

²V. M. Galitskii, S. P. Goreslavskii, and V. F. Elesin, *Zh. Eksp. Teor. Fiz.* **57**, 207 (1969) [*Sov. Phys. JETP* **30**, 117 (1970)].

³P. F. Liao and J. E. Bjorkholm, *Phys. Rev. Lett.* **34**, 1 (1975).

⁴D. Fröhlich, A. Nöhte, and K. Reimann, *Phys. Rev. Lett.* **55**, 1335 (1985).

⁵A. Mysyrowicz, D. Hulin, A. Antonetti, A. Migus, W. T. Masselink, and H. Morkoc, *Phys. Rev. Lett.* **56**, 2748 (1986).

⁶A. VonLehman, D. S. Chemla, G. E. Zinker, and G. P.

Heritage, *Opt. Lett.* **11**, 609 (1986).

⁷K. Tai, G. Hegarty, and W. T. Tsang, *Appl. Phys. Lett.* **51**, 152 (1987).

⁸D. Fröhlich, R. Wille, W. Schlapp, and G. Weimann, *Phys. Rev. Lett.* **59**, 1748 (1987).

⁹B. Fluegel, N. Peyghambarian, G. Olbright, M. Lindberg, S. W. Koch, M. Joffre, D. Hulin, A. Migus, and A. Antonetti, *Phys. Rev. Lett.* **59**, 2588 (1987).

¹⁰M. Lindberg and S. W. Koch, *Phys. Rev. B* **38**, 3342 (1988).

¹¹S. Schmitt-Rink and D. S. Chemla, *Phys. Rev. Lett.* **57**, 2752 (1986); S. Schmitt-Rink, D. S. Chemla, and H. Haug, *Phys. Rev. B* **37**, 941 (1988).

¹²M. Combescot and R. Combescot, *Phys. Rev. Lett.* **61**, 117 (1988).

¹³R. Zimmerman, *Phys. Status Solidi (b)* **146**, 371 (1988).

¹⁴C. Ell, J. F. Müller, K. El Sayed, and H. Haug, *Phys. Rev. Lett.* **62**, 304 (1989); (private communication).

¹⁵W. Knox, J. B. Stark, D. S. Chemla, D. A. B. Miller, and S. Schmitt-Rink, postdeadline paper to the Conference on Ultrafast Phenomena, Kyoto, Japan, 12–15 July 1988 (unpublished).